Int. J. Multiphase Flow, Vol. 1, pp. 103–122. Pergamon Press, 1973. Printed in Great Britain.

THE LOCAL STRUCTURE OF GAS FLUIDIZED BEDS —I. A STATISTICALLY BASED MEASURING SYSTEM

J. WERTHER and O. MOLERUS

Institut für Mechanische Verfahrenstechnik, der Universität Erlangen-Nürnberg, 8520 Erlangen, W. Germany

(*Received* 15 *May* 1973)

Abstract—A system is described for measuring the parameters characterizing the local state of fluidization in beds of arbitrary sizes. This system is based on a miniaturized capacitance probe shaped so as not to disturb the local state of fluidization. Based on a statistical analysis of the signal, the mean bubble pulse duration, the number of bubbles striking the probe per unit time and the local mean bubble rise velocity are measured. The latter is measured by using the cross-correlation technique. From these parameters, further characteristics of the local state of fluidization are derived, in particular the local mean pierced length of bubbles, the local bubble volume fraction and the local bubble gas flow.

1. INTRODUCTION

Gas/solid-fluidized beds are characterized by inhomogeneities known as "bubbles". The existence of these bubbles is advantageous as they lead to rapid mixing of the solids in the bed and high heat transfer rates between the bed and heating or cooling surfaces. On the other hand in the case of a catalytic fluidized bed reactor where the solids in the bed are catalyst particles, bubble formation causes bypassing of the reaction gas, thus considerably reducing the yield of the reactor (Rowe 1967).

The size of the bubbles, the mechanisms of bubble formation and growth, the spatial distribution of the bubbles within the bed and the distribution of the fluidizing gas between the bubble and dense phases determine the properties of a fluidized bed. An exact knowledge of the hydrodynamic properties is thus a prerequisite for complete mastery of fluidization as a process technology. Such knowledge is already available (Hovmand & Davidson 1971) for the special case of the slugging fluidized bed. However, for the general case of the bubbling fluidized bed, where bubble sizes are small compared to the bed diameter, the information is not complete. The reason for this lies in the difficulties associated with current measuring techniques, which have yielded so far only approximate information or information of limited applicability regarding the hydrodynamic properties of fluidized beds.

For example, the measurement of bubble sizes employing photography of bubble eruptions at the bed surface (Geldart 1970/71; Argyriou, List & Shinnar 1971), is certain to be inaccurate since restrictive assumptions are necessary to relate bubble diameters to eruption diameters. The method used by Rowe & Everett (1972a, b, c), of X-raying a bed cross-section has the advantage that the bubbles are not disturbed by the measuring technique. However, this method is limited by two factors. Firstly, the bed dimension is

limited in the direction of ray transmission to about 30 cm by the availability of radiation sources. Secondly, only relatively low fluidizing velocities may be investigated since at higher bubble concentrations individual bubbles may no longer be distinguished clearly. Measurements carried out on two-dimensional beds are only of limited applicability in this connection, although such experiments have yielded valuable insights into individual phenomena such as bubble coalescence. Such data, however, requires amplification and corroboration by corresponding experiments in three-dimensional beds, as has already been pointed out by Grace & Harrison (1968) as well as by Rowe & Everett (1972b).

The measurement of the local hydrodynamic properties in three-dimensional fluidized beds of arbitrary dimensions is possible with capacitive (Morse & Ballou 1951; Bakker 1958; Fukuda, Asaki & Kondo 1967; Kunii, Yoshida & Hiraki 1967; Geldart & Kelsey 1972), optical (Yasui & Johanson 1958; Whitehead & Young 1967), and conductivity probes (Park *et al.* 1969). None of these has gained general acceptance. In most cases this was due to the shapes of the probes which caused destruction of the rising bubbles rather than the determination of the local state of fluidization. Further defects were often due to the too inaccurate treatment and interpretation of the electrical signals as well as the fact that parameters such as bubble frequency or average bubble length are, by themselves, insufficient to draw useful conclusions.

The first goal of the investigations was the development of a probe suitable for local measurements, with a minimum disturbance to the state of fluidization. The second aim was to develop measurement and evaluation techniques to allow measurement of quantities that characterize the local state of fluidization. Such quantities are the gas flow passing as bubbles, the bubble volume fraction, the mean pierced length of a bubble and the mean bubble rise velocity—all obtained as local values.

Bubble development is characterized by its statistical nature, i.e. bubbles rise at random times and proceed to grow by random coalescence. Therefore, the probe registers a stochastic phenomenon and it is necessary that the signal obtained be interpreted stochastically and be analysed with appropriate statistical methods.

Because measuring techniques employing probes have to date repeatedly raised fundamental doubts as to their utility (Argyriou, List & Shinnar 1971; Rowe 1971; Lockett & Harrison 1967; Rowe & Partridge 1965) Part I of this publication presents in detail the development of such a technique. In Part II the application of the technique to the investigation of the spatial distribution of bubbles in a fluidized bed follows.

2. DEVELOPMENT OF THE PROBE

A probe suitable for detection of local variations of porosity with time should:

(a) disturb the state of fluidization as little as possible;
(b) measure local variables;
(c) detect rapid variations in porosity;
(d) possess adequate mechanical strength;
(e) be capable of relocation within the bed, i.e. it should not be fixed at some position;
(f) be compatible with the solids normally encountered in fluidization.

The capacitance probe shown in figure 1 is most compatible with the above requirements, where the capacitor is part of a high frequency oscillator circuit. The temporal variation of the porosity $\varepsilon(t)$ at the capacitor causes a change in the capacitance which in turn results in a proportional d.c. voltage $U(t)$. A reactance converter changes the frequency in the oscillator circuit.

The plate capacitors used by a number of authors such as Morse & Ballou (1951), Bakker (1958), Kunii, Yoshida & Hiraki (1967) and Geldart & Kelsey (1972) are unsuited for exact measurements since their presence significantly changes the local state of fluidization. This has been demonstrated by experiments of the authors described below in detail.

Every object inserted in a fluidized bed disrupts the state of fluidization in its vicinity in some way. The extent of the disturbance depends on the shape and size of the object. Thus, the aim of the development of a suitable probe must be to choose a shape and size to minimize such disturbances. Considerations of this kind led to the development of the needle probe shown in figure 1. The protruding needle forms one pole, while the enclosing metal tube forms the other pole of the capacitor. To investigate the disturbance of the probe on the state of fluidization, the following experimental set-up was used: in a 10-cm dia. bed of glass spheres (mean particle dia. of 180 μm) fluidized by air at a superficial velocity of 11.7 cm/sec, a needle probe was mounted in the center of the tube at a height of 42 cm above the distributor plate. The power spectral density of the probe signal was measured with an ISAC-correlator (Noratom A/S, Norway) with only one probe. The measurement was repeated with a second needle probe mounted 3 cm below the first one. The presence of the lower needle probe did not noticeably alter the shape of the power spectral density function of the upper probe signal. On the other hand, when the lower needle probe was replaced by a plate capacitor with the same dimensions as used by Bakker (1958) the power spectral density changed considerably, indicating that the local state of fluidization was changed by the presence of the plate capacitor. It was thus concluded that a needle probe has no detectable effect on the state of fluidization in its vicinity. This is in agreement with the observations of Rowe & Everett (1972a), where single vertical rods of 6.3 and 3.15 mm dia. had no observable effect on the bubble pattern in freely bubbling beds.

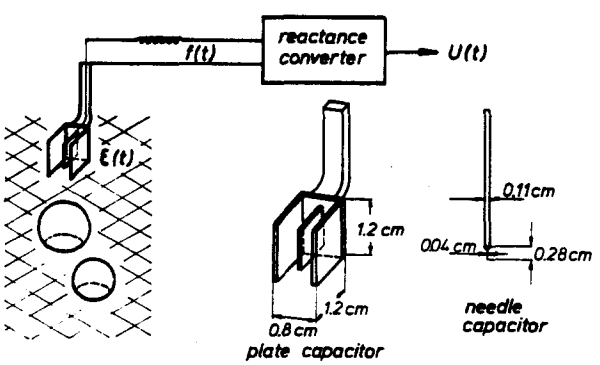

Figure 1. Bubble measurement with capacitive probes. A plate capacitor of the dimensions shown was used by Bakker (1958).

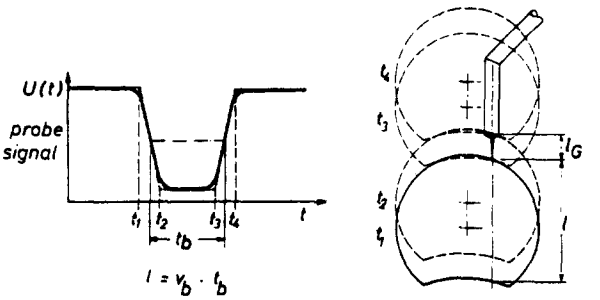

Figure 2. Probe signal when the probe is hit by a rising bubble.

In figure 2 the signal $U(t)$ is shown versus the time for the case when a bubble strikes a probe of short needle length l_G as compared to the bubble dimensions. The bubble generates an electric pulse of duration t_b, which is proportional to the pierced length, l:

$$l = v_b \cdot t_b \qquad [1]$$

where v_b is the rise velocity of the bubble.

The expression

$$t_{ri} = l_G/v_b \qquad [2]$$

for the time of rise of the pulse is justified by an experiment in which the bubble's approach to the probe was simulated in the following way. The probe was slowly dipped into a liquid (cyclohexane) while the output U of the reactance converter was registered. The result is depicted in figure 3. Although the electric field of the needle capacitor passes to infinity, 93 per cent of the total signal amplitude is achieved during the submergence of the probe needle. It is significant that the variation of the voltage is linear during the submergence, except for the liquid adhesion effects brought about by the surface tension peculiar to this experiment. Thus, the bubble pulse is represented in the mathematical model by a trapezoid.

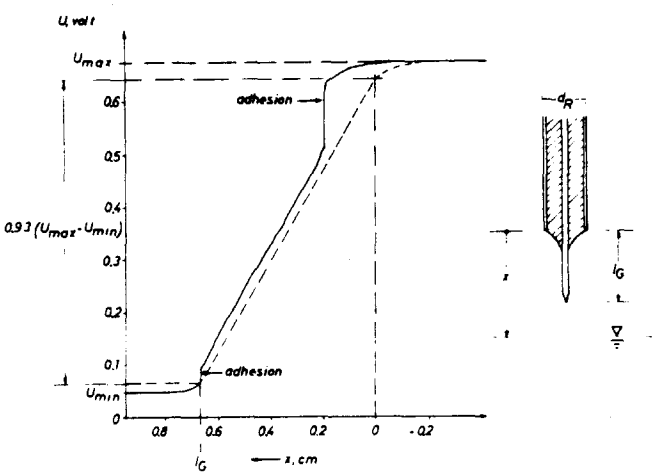

Figure 3. Probe signal when the probe is dipped into a liquid (cyclohexane).

In another experiment the probe was submerged with the axis of the tube parallel to the liquid surface. These experiments indicated that the volume associated with the needle probe is almost equal to the volume of a cylinder with diameter d_R of the probe tube and height l_G of the probe needle.

Finally, the simple shape of the probe allows considerable miniaturization as is shown in figure 4. Since the volume associated with such a miniaturized probe is only about 2.5 mm^3, it is capable of detecting even the smallest bubbles occurring in gas fluidized beds.

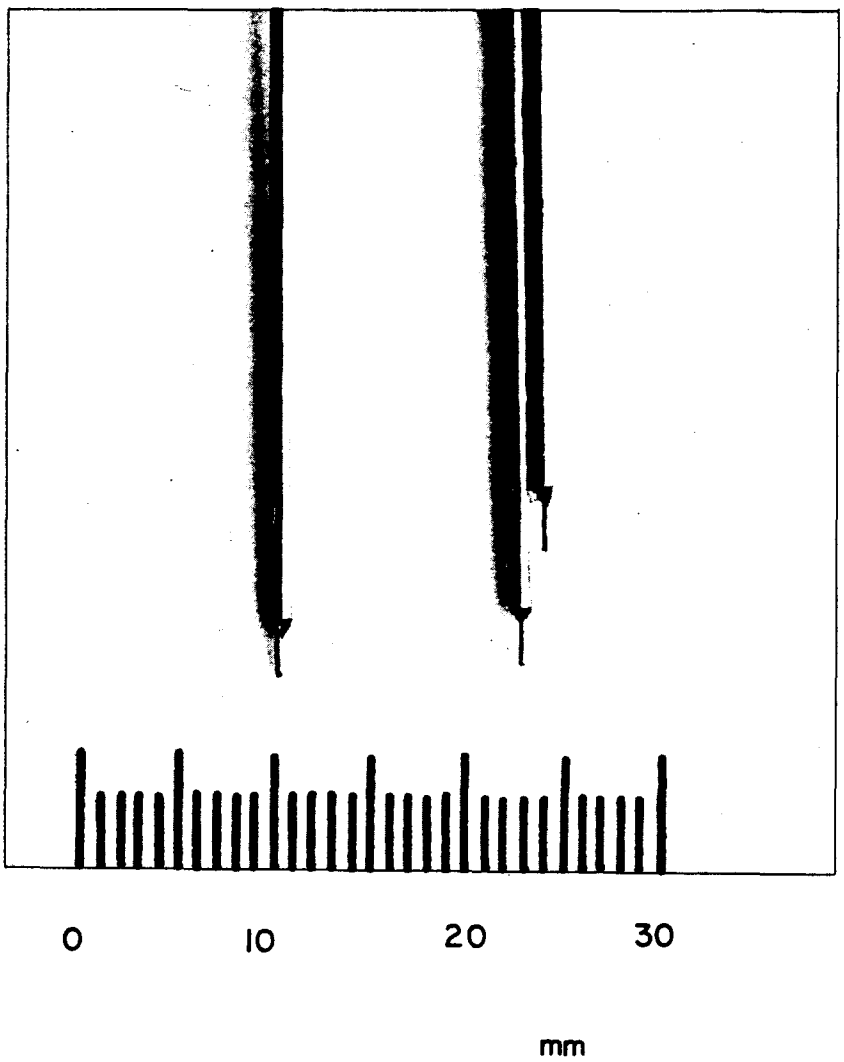

Figure 4. Miniaturized probes (left: single probe, right: double probe for measuring bubble rise velocities).

3. INTERPRETATION OF THE PROBE SIGNAL

The output signal $U(t)$ of the probe contains information on the bubble phase, and on the local porosity variations of the dense phase as indicated in the example of figure 5. In the present investigations only the information about the bubble phase is sought.

It is impossible to process directly the probe signal for determination of the mean duration of the bubble pulses and other information. Instead, the signals due to the bubble pulses and those due to the variations of porosity of the dense phase must first be separated. This discrimination must be based on objective criteria, such that information is neither lost nor distorted.

Since it is expected that the bubble pulses differ significantly in their heights from the amplitudes of the porosity variation, it seems reasonable to attempt a separation of the two parts of the signal by a simple limiting technique. This limiting may be effected by the amplitude discriminator circuit represented in figure 6. Only that part of the signal $U(t)$ that lies below an adjustable reference value U_D is transmitted undistorted, while for other parts of $U(t)$ the signal is blocked and the output is constant U_D. An additional circuit produces a signal more suited for further automatic processing $U''(t)$ in the form of rectangular pulses of constant heights. The duration of such a rectangular pulse is identically t_g for which the discriminator circuit detects the corresponding pulse.

An experiment was conducted to demonstrate that the pulses obtained from the bubbles differ from the ones obtained from the temporal variation of dense phase porosity. The mean number of pulses per unit time κ of the signal $U''(t)$ was obtained by means of an electronic counter, for different levels of the reference voltage U_D. As may be seen in figure 7, the number of pulses rapidly increases as U_D rises from an initial value U_I. The rate of increase then diminishes and the pulse count reaches a stationary value k at U_{II}. Beyond a value U_{III} the pulse count again rises rapidly due to the discriminator circuit, allowing the passage of peaks due to porosity fluctuations in the dense phase. The distribution of the bubble pulse heights therefore exhibits at the value U_{II} a limit which is clearly differentiable from above U_{III}. Thus when U_D is set at a value between U_{II} and U_{III}, the output $U(t)$ of the discriminator circuit contains all bubble pulses but no components due to the porosity fluctuations.

The reference level to effect a satisfactory separation may be estimated from a plot of κ versus U_D. For a large number of experiments a more expeditious procedure is desirable.

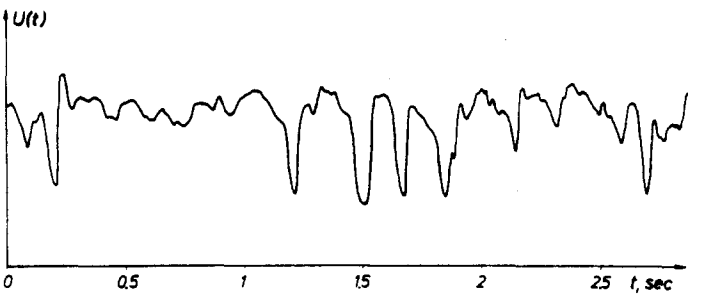

Figure 5. Output of the reactance converter when the probe is placed into a freely bubbling bed.

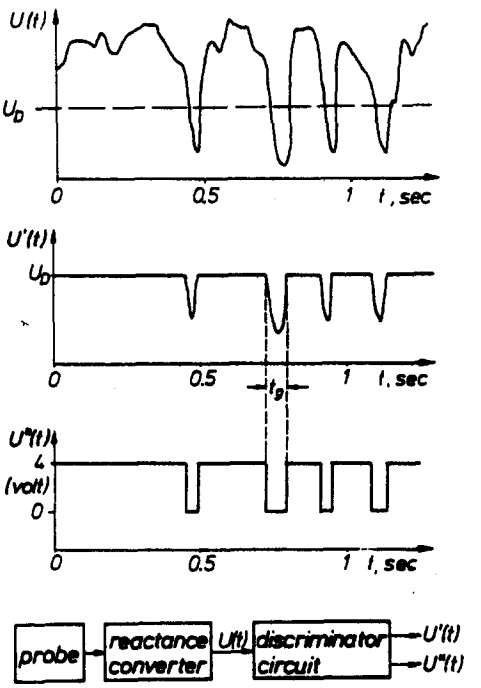

Figure 6. Processing of the probe signal.

Due to the stochastic nature of the signal $U(t)$ the determination of the reference level U_D is impossible by merely considering individual signal elements. It is to be expected that such a determination may be possible using a statistical description of the signal such as the probability distribution of the signal amplitudes. However, in order to determine U_D given a measured amplitude distribution of the probe signal $U(t)$, one requires information on the composition of the signal. Therefore, amplitude distributions are predicted for both parts of the signal on the basis of appropriate mathematical models. By superposition, the distribution for the complete signal is determined.

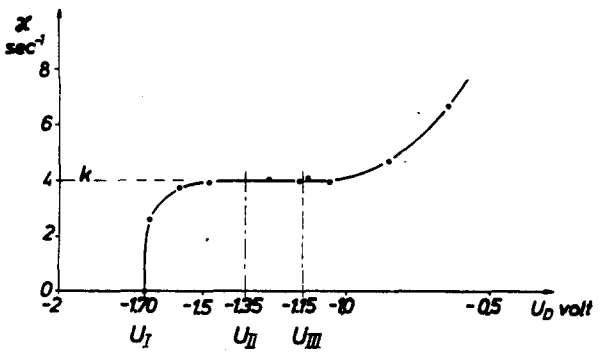

Figure 7. Variation of the mean number of pulses per unit time in the signal $U''(t)$ with the reference voltage U_D of the discriminator circuit (copper powder of mean particle size of 67 μm fluidized by air, gas velocity 8.4 cm/sec, probe located in the center of a 10-cm dia. bed, 8 cm above the distributor).

Let U_1 denote that portion of the signal arising from dense phase porosity fluctuations. U_1 varies stochastically within the bounds $U_{1\,\min}$ and $U_{1\,\max}$ about an expected value $\bar{U}_1$. The component of $U(t)$ arising from the presence of bubbles is denoted U_2. The bubble pulses exhibit heights z such that $z_{\min} \leq z \leq z_{\max}$, and pulse durations t_b ranging from $t_{b\,\min}$ to $t_{b\,\max}$. The corresponding probability density distributions are $q(z)$ and $w(t_b)$, respectively. The mean duration of a bubble pulse is denoted by $\bar{t}_b$

$$\bar{t}_b = \int_{t_{b\,\min}}^{t_{b\max}} t_b w(t_b)\, dt_b. \qquad [3]$$

From the signal $U(t)$, the functions $U_1(t)$ and $U_2(t)$ are constructed by the following definitions: For a probe immersed in a bubble at time t

$$U_1(t) = \bar{U}_1; \quad (\bar{U}_1 - z_{\max}) \leq U_2(t) < \bar{U}_1.$$

For a probe not immersed in a bubble at t

$$U_{1\,\min} \leq U_1(t) \leq U_{1\,\max} \quad \text{and} \quad U_2(t) = \bar{U}_1.$$

The decomposition of the signal $U(t)$ as defined in this way is depicted in figure 8.

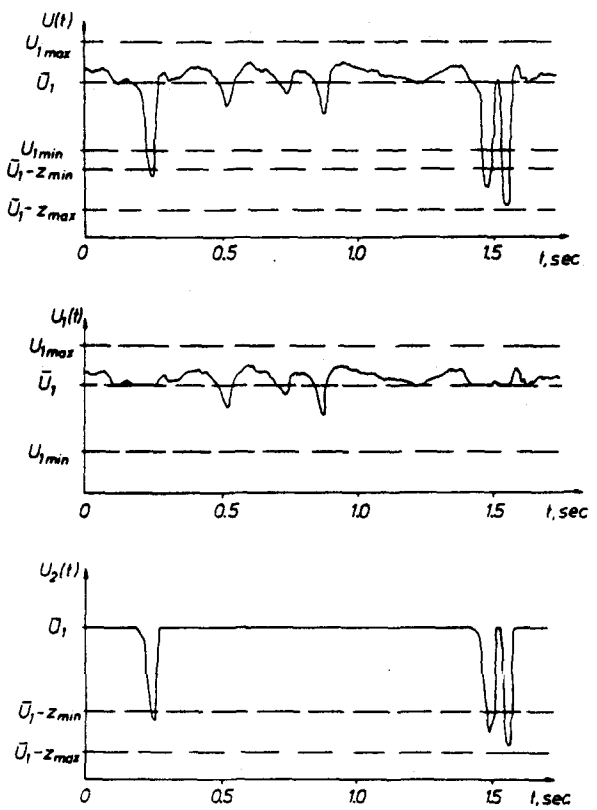

Figure 8. Decomposition of the probe signal into its components U_2 due to bubbles and U_1 due to dense phase porosity fluctuations.

Let $w(U)\,dU$ be the probability that at an arbitrary time t the signal $U(t)$ has a value in the interval U to $U + dU$, with corresponding definitions for the distributions of $w_1(U_1)$ and $w_2(U_2)$.

In order to compute the probability distribution of the amplitude of the signal $U_2(t)$, the shape of the bubble pulse is approximated by trapezoid with a rise time t_r,

$$t_r = l_G/\bar{v}_b \qquad [4]$$

where $\bar{v}_b$ is the mean rise velocity of the bubbles at the point of the probe.

The stochastic process of bubble pulse appearance is described by a Poisson-process, i.e. the probability $P_\zeta(n, \theta)$ that n bubbles strike the probe in the time interval of duration θ is given for stationary bed operation by the Poisson distribution (Gnedenko 1968):

$$P_\zeta(n, \theta) = \frac{(k\theta)^n}{n!} e^{-k\theta}. \qquad [5]$$

Since in the present case only time intervals $\theta = O(t_b)$ are of interest, and since from experiments it is known that bubble pulses occur infrequently namely $k\theta \ll 1$ for $\theta \leq t_{b\max}$, [5] can be simplified as follows:

$$P_\zeta(n, \theta) = \begin{cases} 1 - k\theta & n = 0 \\ k\theta & n = 1 \\ 0 & n \geq 2 \end{cases} \qquad \text{for } k\theta \leq kt_{b\max} \ll 1 \qquad [6]$$

where k is the number of bubbles striking the probe per unit time. Equation [6] adequately describes the stochastic process of the appearance of bubble pulses. Starting from the definition of the function $w_2(U_2)$, using the rules for manipulating compound probabilities, conditional probabilities and unconditional probabilities (see for example Lee 1960) it is possible to compute the probability density distribution $w_2(U_2)$ of the amplitude of the signal $U_2(t)$.

The probability that $U_1(t)$ has a value $U_1(t) = \bar{U}_1$ at time t, is identical to the probability P that at the same time the probe is immersed in a bubble. This probability is

$$P = k(\bar{t}_b + t_r). \qquad [7]$$

One thus arrives at the following expression for the probability density distribution $w_1(U_1)$:

$$w_1(U_1) = [1 - k(\bar{t}_b + t_r)]h(U_1) + k(\bar{t}_b + t_r)\delta(U_1 - \bar{U}_1) \qquad [8]$$

where $\delta(U_1 - \bar{U}_1)$ is the Dirac delta function and $h(U_1)$ is the probability density function of the component U_1 associated with the dense phase porosity fluctuations. According to this superposition rule:

$$U(t) = \begin{cases} U_2(t) & \text{for } U_2(t) \neq \bar{U}_1 \\ U_1(t) & \text{for } U_2(t) = \bar{U}_1 \end{cases} \qquad [9]$$

there results the probability density distribution $w(U)$ of the amplitude of the total signal $U(t)$:

$$w(U) = \begin{cases} 0 & U < \bar{U}_1 - z_{max} \\ k(\bar{t}_b - t_r)q(\bar{U}_1 - U) + 2kt_r \int_{\bar{U}_1 - U}^{z_{max}} \frac{q(z)}{z} dz & \bar{U}_1 - z_{max} \leq U \leq \bar{U}_1 - z_{min} \\ 2kt_r \int_{z_{min}}^{z_{max}} \frac{q(z)}{z} dz & \bar{U}_1 - z_{min} \leq U \leq U_{1\,min} \\ [1 - k(\bar{t}_b + t_r]h(U) + 2kt_r \int_{z_{min}}^{z_{max}} \frac{q(z)}{z} dz & U_{1\,min} \leq U < \bar{U}_1 \\ [1 - k(\bar{t}_b + t_r)]h(U) & \bar{U}_1 < U \leq U_{1\,max} \\ 0 & U_{1\,max} < U \end{cases} \quad [10]$$

where for positive ΔU

$$\lim_{\Delta U \to 0} w(\bar{U}_1 - \Delta U) = [1 - k(\bar{t}_b + t_r)]h(\bar{U}_1) + 2kt_r \int_{z_{min}}^{z_{max}} \frac{q(z)}{z} dz$$

$$\lim_{\Delta U \to 0} w(\bar{U}_1 + \Delta U) = [1 - k(\bar{t}_b + t_r)]h(\bar{U}_1).$$

In figure 9 an amplitude distribution, measured by means of a Hewlett–Packard 3721A correlator is shown for the same experimental conditions as those of figure 7. From the

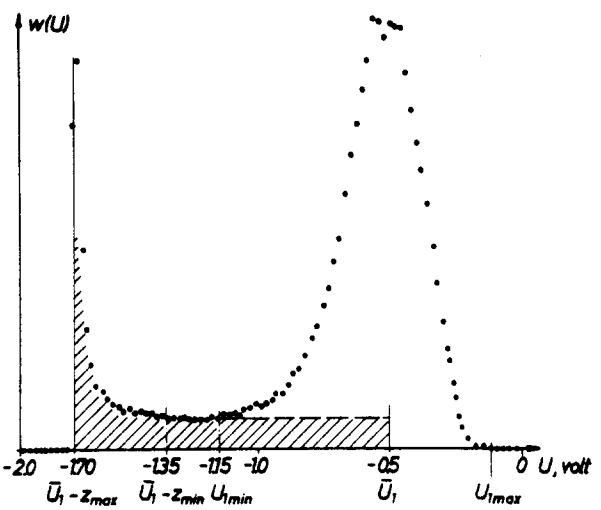

Figure 9. Measured amplitude probability density distribution of the probe signal (same experimental conditions as in figure 7).

measurements of $\kappa(U_D)$ the reference values $U_I = \bar{U}_1 - z_{max}$, $U_{II} = \bar{U}_1 - z_{min}$, $U_{III} = U_{1\,min}$ are used for the amplitude distribution. It is evident that for amplitudes U between U_{II} and U_{III}, the density distribution is constant, as predicted by the theoretical analysis. It is now possible to decide which part of the measured distribution function is to be attributed to the bubble pulses. This part shaded in figure 9, represents 25.8 per cent of the total area under the $w(U)$ curve. Theoretically, this fraction of the area should equal the probability P that at a time t the probe registers a bubble. From the measured values of k, $\bar{t}_b$ and t_r there results, for the present case, a value of $P = 0.223$ which is in good agreement with the fractional area computed above.

Using an approximate pulse height distribution $q(z)$ derived from the measured $\kappa(U_D)$ curve, it is possible to compute from [10] the amplitude density distribution for $U < U_{1\,min}$. The computed and measured distributions $w(U)$ are compared in figure 10. The differences between the curves are primarily due to discrepancies between the actual and assumed bubble pulse shape. Whereas the theory assumes trapezoidal pulses, real pulses exhibit a somewhat smoother variation. Hence the assumption of a trapezoidal form limits the accuracy of the distribution.

The computation of the amplitude distribution of the probe signal and the comparison to experiments has confirmed that measurement of the amplitude distribution of the probe signal $U(t)$ yields an objective criterion for the separation of the signal components. The measured probability density distribution of the amplitude of the probe signal exhibits a region where the density distribution is constant at a low value. Setting the reference level U_D in this region the output signal of the discriminator circuit contains the complete set of bubble pulses. This treatment is admittedly involved, but is necessary for the further processing of the signal.

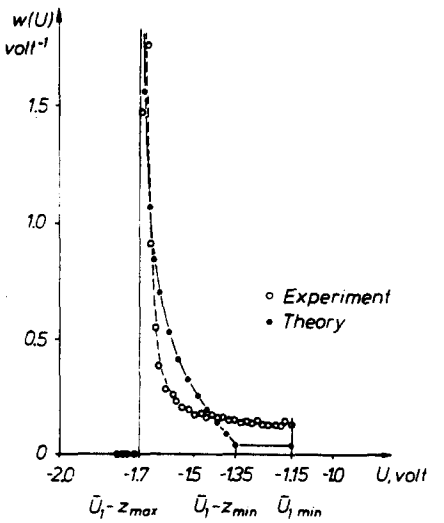

Figure 10. Comparison of measured and computed amplitude probability density distribution (same experimental conditions as in figure 7).

4. METHODS FOR MEASURING LOCAL STATE OF FLUIDIZATION

4.1. *Mean bubble pulse duration* $\bar{t}_b$ *and mean number of bubbles detected by the probe per unit time* k

The output signal $U'(t)$ of the discriminator circuit contains, if U_D is properly set, all bubbles. Since this signal is unsuitable for triggering the electronic counters, the signal $U''(t)$ (cf. figure 6) is used instead to measure the magnitudes of k and $\bar{t}_b$. The arrangement is shown in figure 11. The discriminator feeds the signal $U''(t)$ to two counters for a preselected period T. One counter registers the number n of the bubble pulses within the set period while the other registers the sum of periods t_{gi} corresponding to the bubble pulse durations. For sufficiently large T,

$$k = n/T \quad \text{and} \quad \bar{t}_g = \frac{1}{n}\sum_{i=1}^{n} t_{gi}. \qquad [11, 12]$$

By means of the trapezoidal model of a bubble pulse and an expected pulse height $E[z]$, it is possible to compute the mean bubble pulse duration $\bar{t}_b$ accounting for the discrimination level U_D:

$$\bar{t}_b = \bar{t}_g + t_r\left[2\left(\frac{\bar{U}_1 - U_D}{E[z]}\right) - 1\right]. \qquad [13]$$

It is important that the counter registering the sum of the bubble pulse durations process its input values as rapidly as possible, i.e. have short dead time. The counter used here, Grundig UZ 83, had an adequate switching time of 0.1 msec. The measurement of the mean bubble pulse duration by means of two electronic counters proved to be more accurate than an alternative method (Werther & Molerus 1971) by which the same information was obtained from an auto-correlation function of the signal $U'(t)$. This is because the

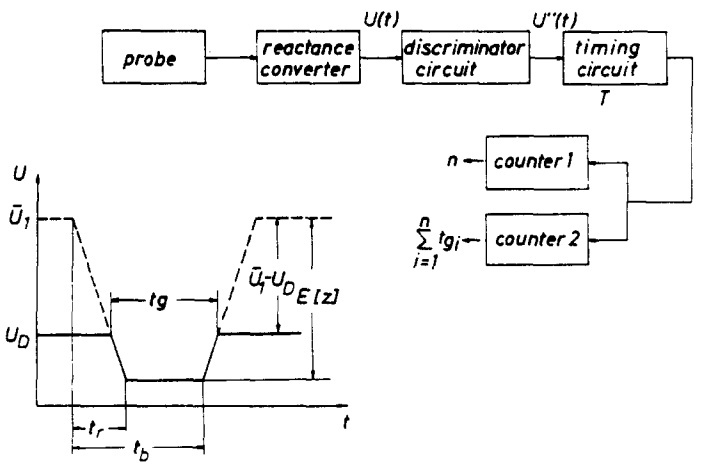

Figure 11. Measurement of the mean bubble pulse duration and of the mean number of bubbles striking the probe per unit time.

measurement of the auto-correlation function is strongly dependent on the shape of the bubble pulses (Werther 1972).

4.2. *The mean rise velocity $\bar{v}_b$ of the bubbles at the point of the probe*

The basic arrangement for the measurement of individual bubble rise velocities is shown in figure 12. Two probes, A and B, were mounted one above the other with a vertical displacement of s. The rising bubble caused a pulse first at the lower then at the higher probe. From the time of the pulse separation t_a, the rise velocity v_b is

$$v_b = s/t_a. \qquad [14]$$

Rowe (1971) has criticized this velocity measurement, stating that it is difficult to identify corresponding bubbles in the signals $U_A(t)$ and $U_B(t)$ due to splitting or coalescence of bubbles between the two probes. To circumvent this difficulty, the probes were separated by a small distance s (i.e. 3.6 mm) as compared to the mean bubble dimension. Consequently, the separation time t_a is short and the probability of bubble coalescence or splitting becomes negligibly small.

For such a small displacement s it is difficult to measure individual pulse separations, because small variations in the shape of the leading and trailing edges of the pulses may lead to significant errors in the magnitude of t_a. However, it is debatable whether single measurements of pulse separations are useful. Prior experimental results show that the instantaneous rise velocity of a bubble depends on a number of random factors:

(1) The rise velocity of an individual bubble is strongly influenced by the proximity and size of neighbouring bubbles, as shown by Godard & Richardson (1969).
(2) During the period immediately prior to coalescence, bubbles about to coalesce influence each other's rise velocity (Rowe 1971; Grace & Harrison 1969; Clift & Grace 1970).
(3) Significant variations in velocity were observed even for single bubbles of the one size

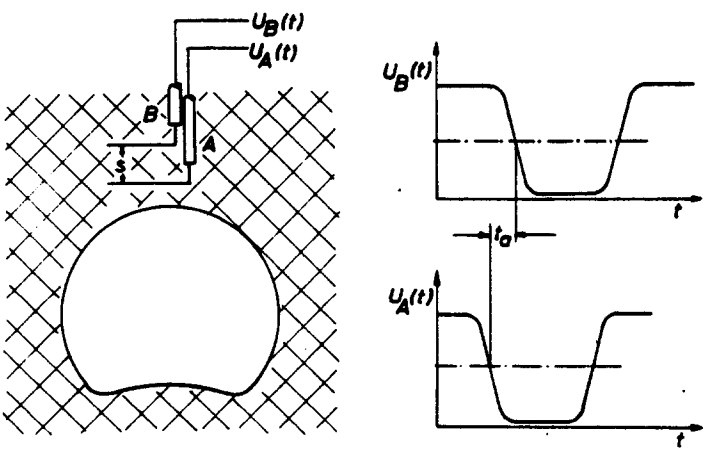

Figure 12. Measurement of the rise velocity of a single bubble.

rising in an infinite medium. This phenomenon is attributed to wake shedding (Rowe & Matsuno 1971).

The fact that the instantaneous rise velocity of a bubble is virtually a stochastic quantity makes the measurement of individual rise velocities pointless. Instead, the local state of fluidization is better described by the mean rise velocity $\bar{v}_b$ of the bubbles at the point of the probe. This is computed from a measurement of the bubble mean rise time, $E[t_a]$:

$$\bar{v}_b = s/E[t_a]. \qquad [15]$$

This bubble mean rise time is measured by means of correlation techniques. These techniques have already found extensive use in the measurement of velocities (Butterfield, Bryant & Dowsing 1961; Miller 1961; Mesch, Daucher & Fritsche 1971), e.g. paper slurry where all elements move at the same velocity and the structure is inherently coherent. The measurement is effected by two probes A and B displaced a distance s in the direction of motion of the structure. These probes yield the electric signals $U'_A(t)$ and $U'_B(t)$ in response to some attribute of the structure. Since it is assumed that all elements move at the same velocity, the two signals are identical except for a constant time displacement:

$$U'_B(t) = U'_A(t - t_a). \qquad [16]$$

Substitution of this relation in the equation defining the cross-correlation function $\phi_{AB}(\tau)$ (Schlitt 1960):

$$\phi_{AB}(\tau) = \lim_{T\to\infty} \frac{1}{2T} \int_{-T}^{+T} U'_A(t)\, U'_B(t + \tau)\, \mathrm{d}t, \qquad [17]$$

shows that the cross-correlation function $\phi_{AB}(\tau)$ is in this case merely an autocorrelation function $\phi_{AA}(\tau)$ displaced by the time t_a:

$$\phi_{AB}(\tau) = \phi_{AA}(\tau - t_a). \qquad [18]$$

Since the auto-correlation function exhibits its maximum at $\tau = 0$ it follows that $\phi_{AB}(\tau)$ exhibits its maximum at $\tau = t_a$. The position of the maximum of the measured cross-correlation function hence yields the desired time displacement t_a from which, for a known probe displacement s, the velocity of the structure may be deduced.

In the case of the rise velocity of bubbles in a fluidized bed, the pulse separation t_a is stochastic, and measurements show that the cross-correlation function is not a time-displaced auto-correlation function (figure 13). Furthermore, it is doubtful whether the position of the maximum of the cross-correlation function yields the desired mean time displacement $E[t_a]$. The position of the maximum was therefore calculated. This calculation is based on the experimental observation that the time delay τ^* at which the maximum occurred was independent of whether the signals $U'(t)$ or $U''(t)$ were cross-correlated (cf. figure 6). Therefore, the mathematical model uses the signal of simpler shape $U''(t)$. The signals $U''_A(t)$ and $U''_B(t)$ consisting of random series of rectangular pulses of stochastically varying duration but of constant height, are cross-correlated according to [17]. The pulse separations t_a of the corresponding pulses vary stochastically between the

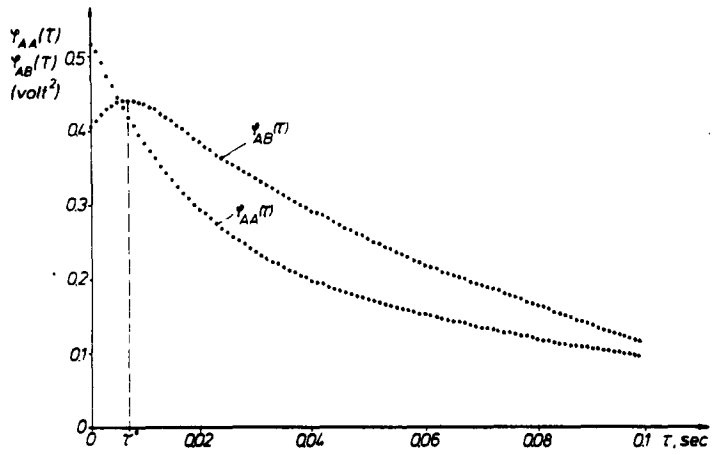

Figure 13. Comparison of measured auto-correlation and cross-correlation function.

limits $t_{a\min}$ and $t_{a\max}$. The computations, given in detail by Werther (1972), show that the separation time τ^* where the maximum occurs, depends on the form of the distribution of the pulse separations $q_a(t_a)$. Corresponding measurements have shown that the distributions $q_a(t_a)$ are skewed. In that case it follows that

$$\tau^* = t_{a\,\mathrm{med}}$$

where the median value $t_{a\,\mathrm{med}}$ is defined by

$$\int_{t_{a\min}}^{t_{a\mathrm{med}}} q_a(t_a)\,\mathrm{d}t_a = 0.5. \qquad [19]$$

The difference between $t_{a\,\mathrm{med}}$ and the expected value $E[t_a]$ may be neglected, as shown by the evaluation of distributions $q_a(t_a)$. Hence, the position of the maximum of the cross-correlation function of the two probe signals is used to estimate the mean time $E[t_a]$ for the bubbles to rise from probe A to probe B. Using this value, the local mean rise velocity of the bubbles at the position of the probe is determined.

4.3. *Description of the local state of fluidization by the parameters $E[l]$, ε_b and $\dot{V}_b$*

The three parameters k, $\bar{t}_b$ and $\bar{v}_b$ do not directly yield a satisfactory description of the bed. However, they are used in deriving significant characteristics of the local state of fluidization.

Mean pierced length of bubbles, $E[l]$. It is assumed that the duration t_b of a bubble pulse and the instantaneous rise velocity of the corresponding bubble are stochastically independent. The statistical mean pierced length l corresponding to a pulse duration t_b is then

$$l \cong \int_{v_{b\min}}^{v_{b\max}} v_b t_b q_v(v_b)\,\mathrm{d}v_b \qquad [20]$$

$$l = E[v_b]t_b \qquad [21]$$

where $q_v(v_b)$ is the number density distribution of the rise velocities at the point of the probe. Measurements of the $q_a(t_a)$ distribution have shown that it is possible to approximate the expected value $E[v_b]$ by the mean velocity $\bar{v}_b$, determined by means of correlation measurements. Thus

$$l = \bar{v}_b t_b \qquad [22]$$

and the expected value $E[l]$ of the pierced lengths is

$$E[l] = \bar{v}_b \bar{t}_b. \qquad [23]$$

The mean pierced length $E[l]$ is a measure for the mean size of bubbles at the point of the probe, providing bubbles rise randomly. The exact relationship between the distribution of the pierced lengths and the bubble size distribution will be treated in a separate publication (Werther 1973). As an example, figure 14 shows the growth of the mean pierced length with increasing height h above the distributor as measured in a cylindrical fluidized bed with a diameter of 10 cm. The hydrodynamic interpretation of these measurements as well as of the experimental results depicted in figures 15 and 16 follow in Part II of this paper.

The local bubble volume fraction, ε_b. A volume element of the fluidized bed at the point of the probe contains on a time-averaged basis, a fraction ε_b of gas bubbles. This fraction equals the ratio of the time in which the probe registers bubbles, to the total time for which measurements have been made T:

$$\varepsilon_b = \lim_{T \to \infty} \frac{1}{T} \sum_{i=1}^{n} t_{bi} \qquad [24]$$

where n = number of bubbles registered in time T. It follows

$$\varepsilon_b = k\bar{t}_b. \qquad [25]$$

As an example, figure 15 shows the local bubble volume fraction versus the radial distance from the centre-line of a cylindrical fluidized bed of 10 cm dia. The measurements refer to a section 8 cm above the distributor.

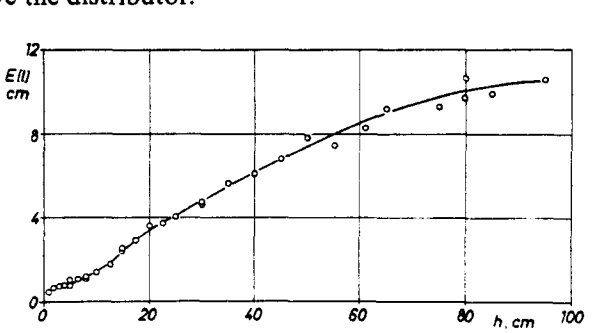

Figure 14. Variation of the local mean bubble pierced length with height above the distributor (quartz sand of mean particle size of 83 μm fluidized by air in a 10-cm dia. bed, probe located in the column axis, gas velocity 9 cm/sec).

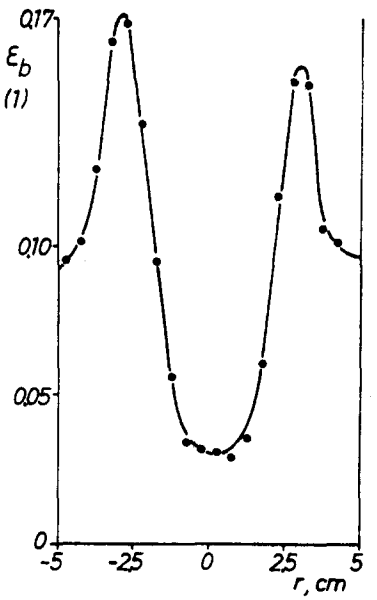

Figure 15. Variation of the local bubble volume fraction with radial displacement of the probe from the vessel center-line (quartz sand of mean particle size of 83 μm fluidized by air in a 10-cm dia. bed, probe located 8 cm above the distributor, gas velocity 9 cm/sec).

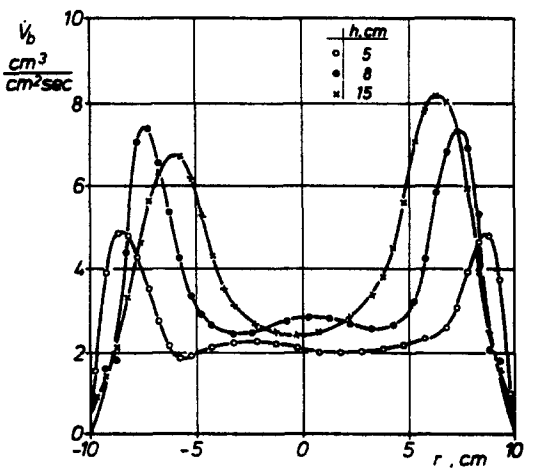

Figure 16. Variation of the local bubble gas flow with radial displacement of the probe from the vessel center-line for different heights h above the distributor (quartz sand of mean particle size of 83 μm fluidized by air in a 20-cm dia. bed, gas velocity 9 cm/sec).

The local bubble gas flow, $\dot{V}_b$. The mean gas volume flowing through a surface element dF per unit area and unit time is given by

$$\dot{V}_b = \lim_{T\to\infty} \frac{1}{T\,dF} \sum_{i=1}^{n} l_i\,dF \qquad [26]$$

from which it follows that $\dot{V}_b = k\bar{l}_b\bar{v}_b$. [27]

It is significant that in determining the local bubble gas flow no assumptions have been made concerning the shape of the bubbles. In figure 16 experimental results are shown of the local bubble gas flow versus the distance r from the bed centre-line. The height above the distributor is a parameter. The results indicate the accuracy of the measuring technique described here.

5. SUMMARY AND CONCLUSIONS

A system for measuring the parameters describing the local state of fluidization is developed. The system is based on a capacitive probe shaped such as not to disturb the local state of fluidization. Extensive miniaturizations ensure that even bubbles of only a few millimeters diameter are detected.

The separation of the component of the probe signal due to bubbles striking the probe from the component due to random fluctuations of the dense phase porosity is achieved. This separation is based on the statistical nature of the phenomenon and on the measurement of the probability density distribution of the amplitude of the probe signal. After separating the signal, by means of a discriminator circuit, the mean bubble pulse duration $\bar{l}_b$ and the mean number k of bubbles striking the probe per unit time are measured using two electronic counters. The local mean bubble rise velocity $\bar{v}_b$ is obtained from the cross-correlation of the signals from two probes arranged one above the other.

From the parameters k, $\bar{l}_b$ and $\bar{v}_b$ further characteristics of the local state of fluidization are derived, in particular, the local mean pierced length of bubbles $E[l]$, the local bubble volume fraction ε_b, and the local bubble gas flow, $\dot{V}_b$.

Selected examples of experimental measurements show that the above constitutes a complete measuring system capable of accurate investigation of fluidized beds of arbitrary dimensions. In Part II of this paper an investigation of the spatial distribution of bubbles in fluidized beds of various sizes is carried out using this measuring system.

Acknowledgement—The authors thank the Deutsche Forschungsgemeinschaft (DFG) for financial support of this work.

REFERENCES

ARGYRIOU, D. T., LIST, H. L. & SHINNAR, R. 1971 Bubble growth by coalescence in gas fluidized beds. *A.I.Ch.E. J.* **17**, 122–131.

BAKKER, P. J. 1958 Porosity measurements in a fluidized bed. Ph.D. Thesis, TH Delft.

BUTTERFIELD, M. H., BRYANT, G. F. & DOWSING, J. 1961 A new method of strip-speed measurement using random-waveform correlation. *Trans. Soc. Inst. Technol.* **13**, 111–119.

CLIFT, R. & GRACE, J. R. 1970 Bubble interaction in fluidized beds, *Chem. Engng Progr. Symp. Ser.* **66**, 14–34.

FUKUDA, M., ASAKI, Z. & KONDO, Y. 1967 On the nonuniformity in fluidized bed. *Mem. Fac. Eng. Kyoto Univ.* **29**, 287–299.

GELDART, D. 1970/71 The size and frequency of bubbles in two- and three-dimensional gas-fluidized beds. *Powder Tech.* **4**, 41–61.

GELDART, D. & KELSEY, J. R. 1972 The use of capacitance probes in gas fluidized beds. *Powder Tech.* **6**, 45–60.

GNEDENKO, B. W. 1968 *Lehrbuch der Wahrscheinlichkeitsrechnung*. Akademie-Verlag.

GODARD, K. & RICHARDSON, J. F. 1969 Bubble velocities and bed expansions in freely bubbling fluidized beds. *Chem. Engng Sci.* **24**, 663–683.

GRACE, J. R. & HARRISON, D. 1968 The distribution of bubbles within a gas-fluidized bed. *Instn. Chem. Engrs Symp. Ser.* **30**, 105–114.

GRACE, J. R. & HARRISON, D. 1969 The behaviour of freely bubbling fluidized beds. *Chem. Engng Sci.* **24**, 497–509.

HOVMAND, S. & DAVIDSON, J. F. 1971 Slug flow reactors. In: *Fluidization*, p. 193 (Eds J. F. Davidson & D. Harrison). Academic Press.

KUNII, D., YOSHIDA, K. & HIRAKI, J. 1967 The behaviour of freely bubbling fluidized beds. *Proceedings of the International Symposium on Fluidization*, p. 243. Eindhoven.

LEE, Y. W. 1960 *Statistical Theory of Communication*. Wiley.

LOCKETT, M. J. & HARRISON, D. 1967 The distribution of voidage fraction near bubbles rising in gas-fluidized beds. *Proceedings of the International Symposium on Fluidization*, p. 257. Eindhoven.

MESCH, F., DAUCHER, H. H. & FRITSCHE, R. 1971 Geschwindigkeitsmessung mit Korrelationsverfahren. *Messtechnik* **7**, 152–170.

MILLER, R. J. 1961 Air and space navigation system uses cross-correlation techniques. *Electronics* **50**, 55–70.

MORSE, R. D. & BALLOU, C. O. 1951 The uniformity of fluidization, its measurement and use. *Chem. Engng Progr.* **47**, 199–211.

PARK, W. H., KANG, W. K., CAPES, C. E. & OSBERG, G. L. 1969 The properties of bubbles in fluidized beds of conducting particles as measured by an electroresistivity probe. *Chem. Engng Sci.* **24**, 851–870.

ROWE, P. N. & PARTRIDGE, B. A. 1965 An X-ray study of bubbles in fluidized beds. *Trans. Instn. Chem. Engrs* **43**, 157–190.

ROWE, P. N. 1967 General lecture. *Proceedings of the International Symposium on Fluidization*, p. 11. Eindhoven.

ROWE, P. N. 1971 Experimental properties of bubbles. In: *Fluidization*, p. 121 (Eds J. F. Davidson & D. Harrison). Academic Press.

ROWE, P. N. & MATSUNO, R. 1971 Single bubbles injected into a gas fluidized bed and observed by X-rays. *Chem. Engng Sci.* **26**, 923–940.

ROWE, P. N. & EVERETT, D. J. 1972a Fluidized bed bubbles viewed by X-rays, Part I—Experimental details and the interaction of bubbles with solid surfaces. *Trans. Instn. Chem. Engrs* **50**, 42–60.

ROWE, P. N. & EVERETT, D. J. 1972b Fluidized bed bubbles viewed by X-rays. Part II—The transition from two to three dimensions of undisturbed bubbles. *Trans. Instn. Chem. Engrs* **50**, 49–63.

ROWE, P. N. & EVERETT, D. J. 1972c Fluidized bed bubbles viewed by X-rays, Part III—Bubble size and number when unrestrained three-dimensional growth occurs. *Trans. Instn. Chem. Engrs* **50**, 55–70.

SCHLITT, H. 1960 *Systemtheorie für regellose Vorgänge*. Springer.

WERTHER, J. & MOLERUS, O. 1971 Autokorrelation und Kreuzkorrelation zur Messung lokaler Blasengrößen und -aufstiegsgeschwindigkeiten in realen Gas/Feststoff-Fließbetten, *Chemie-Ing.-Techn.* **43**, 271–281.

WERTHER, J. 1972 Experimentelle Untersuchungen zur Hydrodynamik von Gas/Feststoff-Wirbelschichten. Dissertation, Univ. Erlangen-Nürnberg.

WERTHER, J. 1973 Bubbles in gas fluidized beds, to be published.

WHITEHEAD, A. B. & YOUNG, A. D. 1967 Fluidization performance in large scale equipment: Part II. *Proceedings of the International Symposium on Fluidization*, p. 294. Eindhoven.

YASUI, G. & JOHANSON, L. N. 1958 The characteristics of gas pockets in fluidized beds. *A.I.Ch.E. J.* **4**, 445–460.

Sommaire—On décrit un système de mesure des paramètres qui caractérisent l'état local de fluidité dans des bains de grandeurs arbitraires. Ce système est fondé sur une sonde de capacité miniaturisée de forme telle qu'elle ne dérangera pas l'état local de fluidité. Sur la base d'une analyse statistique du signal, on mesure la durée moyenne d'impulsion d'une bulle, le nombre de bulles qui font contact avec la sonde par unité de temps et la vélocité moyenne locale d'élévation de bulle. Cette dernière est mesurée par la technique de corrélation croisée. De ces paramètres on dérive d'autres caractéristiques de l'état local de fluidité, et en particulier la longueur locale moyenne de bulles éclatées, la fraction de volume de bulle locale et l'écoulement local de la bulle de gaz.

Zusammenfassung—Ein System zur Messung der für den lokalen Fluidisationszustand charakteristischen Größen wird beschrieben. Grundlage des Meßsystems, das für Fließbetten beliebiger Abmessungen verwendbar ist, ist ein miniaturisierter kapazitiver Meßwertgeber, der so geformt ist, daß durch seine Anwesenheit der lokale Fluidisationszustand nicht gestört wird. Auf der Grundlage einer statistischen Analyse des Gebersignals durch Messung der Wahrscheinlichkeitsdichteverteilung der Signalamplituden können die mittlere Anzahl der den Geber pro Zeiteinheit treffenden Blasen, die mittlere Blasenimpulsdauer und die lokale mittlere Blasenaufstiegsgeschwindigkeit gemessen werden, wobei die letztere Größe mit Hilfe der Kreuzkorrelationsmeßtechnik bestimmt wird. Aus diesen Meßgrößen werden weitere für den lokalen Fluidisationszustand charakteristische Größen abgeleitet, wie die lokale mittlere Blasendurchstoßlänge, der lokale Blasenvolumenanteil und der lokale, in Form von Blasen transportierte Gasstrom.

Резюме—Описывается система измерения параметров характеризующих местное состояние псевдоожижения слоев выборочных размеров. Эта система основана на емкостном зонде уменьшенных габаритов такой формы, которая не нарушала бы местного состояния флюидизации. На основании статистического анализа сигнала измеряются: средняя продолжительность импульса иузырька, количество пузырьков ударяющихся об зонд на единицу времени и средняя местная скорость появления пузырька. Последнее измеряется методом взаимной корреляции. По этим параметрам получают добавочные характеристики местного состояния флюидизации, в частности местную среднюю длину пересечения пузырьков, местный относительный объем пузыръков и местное течение иузырьков газа.